

The Evolution of MRI of the Prostate: The Past, the Present, and the Future

Francesco Giganti^{1,2}
 Andrew B. Rosenkrantz³
 Geert Villeirs⁴
 Valeria Panebianco⁵
 Armando Stabile^{2,6}
 Mark Emberton^{2,7}
 Caroline M. Moore^{2,7}

Keywords: consensus guidelines, history, MRI, prostatic neoplasms

doi.org/10.2214/AJR.18.20796

Received October 17, 2018; accepted after revision February 5, 2019.

F. Giganti is funded by the University College London (UCL) Graduate Research Scholarship and the Brahm PhD scholarship in memory of Chris Adams. A. B. Rosenkrantz receives royalties from Thieme Medical Publishers. M. Emberton receives research support from University of College London Hospital/UCL UK National Institutes of Health Research (NIHR) Biomedical Research Centre.

¹Department of Radiology, University College London Hospital NHS Foundation Trust, London, United Kingdom.

²Division of Surgery and Interventional Science, University College London, 3rd Fl, Charles Bell House, 43-45 Foley St, London W1W 7TS, United Kingdom. Address correspondence to F. Giganti (f.giganti@ucl.ac.uk).

³Department of Radiology, NYU Langone Health, New York, NY.

⁴Department of Radiology and Nuclear Medicine, Ghent University Hospital, Ghent, Belgium.

⁵Department of Radiological Sciences, Oncology, and Pathology, Sapienza University of Rome, Rome, Italy.

⁶Department of Urology, Division of Experimental Oncology, Vita-Salute San Raffaele University, Milan, Italy.

⁷Department of Urology, University College London Hospital NHS Foundation Trust, London, United Kingdom.

AJR 2019; 213:1–13

0361–803X/19/2132–1

© American Roentgen Ray Society

OBJECTIVE. The purpose of this article is to discuss the evolution of MRI in prostate cancer from the early 1980s to the current day, providing analysis of the key studies on this topic.

CONCLUSION. The rapid diffusion of MRI technology has meant that residual variability remains between centers regarding the quality of acquisition and the quality and standardization of reporting.

It has been nearly 40 years since the first study of MRI of the prostate gland was performed by Steyn and Smith in 1982 [1]. Since then, remarkable advances have occurred in MRI technology, including the introduction of dynamic contrast-enhanced (DCE), DWI, and spectroscopic MRI. Image quality has dramatically improved with the introduction of high-field-strength magnets and phased-array coils [2]. This has improved the accuracy of this technique in detecting clinically significant prostate cancer (PCa) to help in treatment planning and to detect early recurrence.

Data from the PROMIS (Prostate MRI Imaging Study) [3] and PRECISION (Prostate Evaluation for Clinically Important Disease: Sampling Using Image-guidance Or Not) study groups [4] suggest that MRI will have an important role in improving the yield of clinically significant PCa as well as an important role in mitigating overdiagnosis of clinically unimportant disease [5–7].

Extensive literature has described the diagnosis of PCa with the use of MRI, although the reported diagnostic performance of MRI in detection, localization, and local staging vary greatly. This is partly because of heterogeneity in protocols and other aspects related to performing MRI, which in turn reflect the continuous evolution of this technique over time. Thus, the purpose of the present article is to provide an overview of the application of MRI in PCa, from its first use in humans to its present-day use, and to describe future directions of prostate MRI.

The Past: How We Started

The first transperineal ultrasound examination of the prostate was published in 1963, but the image quality associated with this examination was very poor [8]. The first clinical application of 3.5-MHz transrectal ultrasound (TRUS) of the prostate occurred in 1971 and provided new opportunities in the field of prostate imaging [9]. However, imaging techniques such as ultrasound or CT remained unsatisfactory for the identification and characterization of PCa. As an example, Price and Davidson [10] reported in 1979 that the focal obliteration of soft-tissue planes, a common finding in extraprostatic disease, was not distinguishable between benign and malignant disease.

In 1971, the application of MRI in the diagnosis of cancer was first explored by Damadian [11] in six normal tissue samples and two malignant solid tumors in the rat. Malignant tissues could be differentiated according to the T1 and T2 relaxation times, as such, parameters were outside the range of values when compared with the normal tissues.

In 1982, Steyn and Smith [1] reported their initial findings for prostate MRI performed for 25 men with use of a four-coil, air-cored magnetic ring with a static magnetic field of 0.04 T and a slice thickness of 17.53 mm. Twenty men had benign prostatic hyperplasia (BPH), and PCa was observed in five men after surgery (Fig. 1). Steyn and Smith were the first to report the MRI appearance of such conditions, and they concluded that MRI had potential in the management of PCa.

One year later, Hricak et al. [12] used MRI to investigate the anatomy of and patholog-

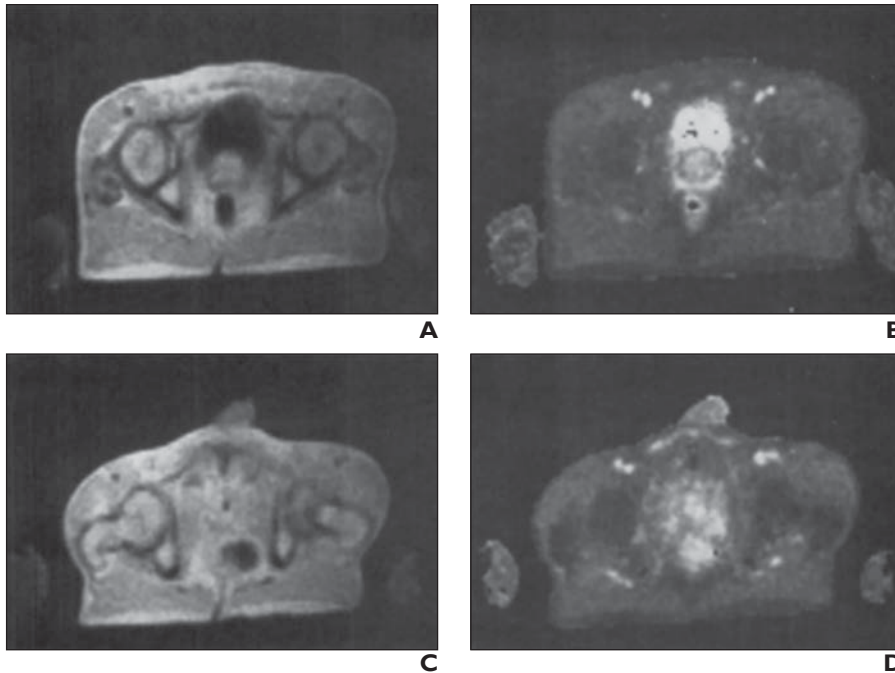


Fig. 1—Images of one man with benign prostatic hyperplasia (BPH) and one man with prostate cancer (PCa). (Reprinted from Steyn JH, Smith FW. Nuclear magnetic resonance imaging of the prostate. *Br J Urol* 1982; 54:726–728, © 1982 British Association of Urological Surgeons, with permission from Wiley and Sons)

A, Proton density-weighted MR image shows BPH with prostate outlined between bladder and rectum. **B**, T1-weighted MR image of benign hyperplasia shows bladder urine (white area in front of prostate) with very long T1 time. **C**, Proton density-weighted MR image shows section of PCa with extension seen posteriorly on right. **D**, T1-weighted MR image shows section of PCa with scattered areas of longer relaxation time.

ic findings for the pelvis in men, including nine men with BPH, nine with PCa, and one with a lymphocele after surgery. MRI enhanced the ability of imaging to provide images in three planes (axial, sagittal, and coronal) to allow accurate volumetric assessment and to assess extension of the malignancy into periprostatic adipose tissue. The major limitation of their study was the inability of the technique to differentiate between a neoplastic nodule and chronic prostatitis. A 0.35-T MRI system was used with an elliptical body producing 7-mm-thick T1- and T2-weighted images with a 3-mm gap between adjacent imaging planes, and T1- and T2-weighted spin-echo sequences were applied.

In 1983, Bryan et al. [13] used a 0.15- or 0.3-T system to obtain T1- and T2-weighted images of four men with PCa and one with BPH, and they reported that PCa had an inhomogeneous appearance on MRI. However, MRI was too expensive to be used as a screening method.

One year later, Buonocore et al. [14] performed clinical and in vitro MRI of the prostate for 10 men. Their results were similar to those of Hricak et al. [12] in that the normal prostate had homogeneous intermediate signal patterns on both T1- and T2-weighted images. PCa and the invasion of seminal vesicles were better seen on T2-weighted images.

In 1985, Poon et al. [15] aimed to determine the optimal pulse sequence for prostatic imaging and to investigate the ability of MRI to distinguish BPH from PCa. The MRI system that was used was a 0.15-T scanner with a body coil. Among the different sequences with different MRI parameters, a dedicated 3D anisotropic imaging set with contiguous 17-mm-thick axial sections (acquired in 10 minutes) was obtained by the investigators, as were 2D single-section sequences with a thickness of 1.5 cm (Figs. 2 and 3). Of interest, Poon and colleagues reported that a 2-hour examination time was set as the upper limit for each individual included in the study, given that it was not possible to perform an exhaustive study of

all techniques for each patient. They could not duplicate the previous results of Hricak et al. [12] and could not differentiate patients with BPH or PCa from normal study participants without symptoms.

In 1987, Hricak et al. [16] published the first descriptive study of the appearance of the prostate gland and periprostatic structures on MRI. Fifty-five men with benign and malignant prostate and bladder disorders were reviewed retrospectively, and the authors discussed the technical requirements (TR/TE, slice thickness, and other parameters) for a scan of diagnostic quality [16]. The participants underwent scanning performed with a 0.35- or 1.5-T system and different body coils (elliptical or quadrate). Multiplanar T1- and T2-weighted images with different TR and TE values were performed for most of the men included in the study. Different slice thicknesses and gaps were also applied. The authors showed how the anatomic structures could be seen when different planes and MR parameters were used.

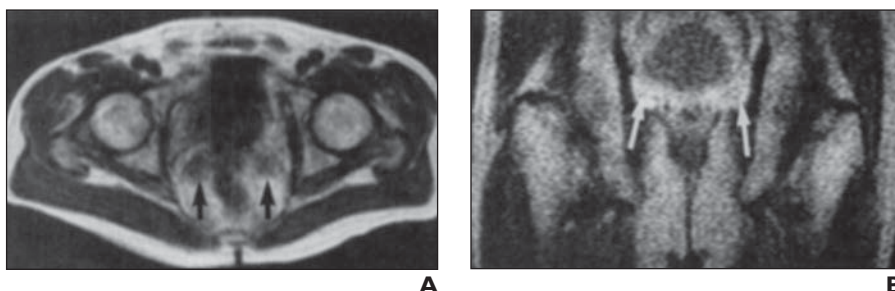


Fig. 2—Man with normal seminal vesicle. (Reprinted from Poon PY, McCallum RW, Henkelman MM, et al. Magnetic resonance imaging of the prostate. *Radiology* 1985; 154:143–149, with permission from the Radiological Society of North America) **A** and **B**, Transverse MR image obtained using 3D anisotropic technique (**A**) and coronal MR image obtained using spin echo of 60/2000 (**B**) show normal seminal vesicle (arrows).

Prostate MRI: Past, Present, and Future



Fig. 3—Man with normal prostate. (Reprinted from Poon PY, McCallum RW, Henkelman MM, et al. Magnetic resonance imaging of the prostate. *Radiology* 1985; 154:143–149, with permission from the Radiological Society of North America)

A and B, Transverse MR image obtained using spin echo (SE) of 120/2000 (**A**) and coronal MR image obtained using SE of 60/2000 (**B**) show bright rim (arrows) around prostate. Corpus cavernosum penis (curved arrow, **B**) is also very bright.

C, Coronal image obtained using SE of 30/500 shows that bright rim in **A** and **B** is not result of layer of fat around prostate because this image shows that pelvic fat is very bright but reveals no periprostatic rim.

Toward Multiparametric Imaging

The MRI protocol currently used for prostate imaging is called multiparametric MRI (mpMRI) because it consists of a combination of T2-weighted imaging, DWI, and DCE-MRI. The importance of DWI has been more widely recognized over time, whereas spectroscopic MRI has declined in popularity [17, 18]. The first applications of MRI for the prostate gland were based on T1- and T2-weighted imaging only, but additional tools, such as DCE-MRI, spectroscopic MRI, and DWI, were developed in the 1990s.

Dynamic contrast-enhanced MRI—In 1993, Mirowitz et al. [19] were the first to report the impact of contrast enhancement on PCa staging (Fig. 4). They concluded that the use of gadolinium was not warranted for routine staging of PCa but could be helpful in assessing seminal vesicles.

Two years later, Brown et al. [20] reported the improved detection of PCa after dynamic acquisition (i.e., acquisition of baseline im-

ages without contrast enhancement, followed by rapid acquisition of a series of images over time) of IV gadolinium (0.2 mL/kg), acquiring 19 contiguous sections in the axial plane (slice thickness, 8 mm) over 3.48 minutes and additional delayed contrast-enhanced images (8 minutes after injection). They concluded that dynamic bolus contrast enhancement could be useful to evaluate tumor margins.

After these initial studies, the use of contrast medium in prostate MRI has seen rapid developments in data acquisition methods, with rapid series of images continuously acquired after bolus administration of contrast medium over time [21–23].

Spectroscopic MRI—The first study of spectroscopic MRI of the prostate was published in 1988 by Sillerud et al. [24]. These authors detected citrate in the prostate, analyzing citrate signals from normal rat tissue and benign hypertrophic human prostate tissue in vitro and from the normal in vivo prostate

tissue of a healthy human volunteer. In 1995, Kurhanewicz et al. [25] determined whether citrate levels detected by spectroscopy could reliably discriminate regions of PCa from healthy peripheral zone tissue and BPH. They observed that the citrate levels were lower in patients with PCa than in patients with BPH or men with normal peripheral zone prostate tissue, with patients with PCa having a lower ratio of the mean (\pm SD) citrate level to peak creatine plus choline levels (0.67 ± 0.17), compared with patients with BPH (1.2 ± 0.29) and men with normal peripheral zone prostate tissue (1.46 ± 0.28) ($p < 0.05$).

Despite the initial excitement about spectroscopic MRI, this technique has now fallen out of favor for PCa assessment. A multicenter study [26] showed no incremental value of spectroscopic MRI over MRI for men with relatively low-volume and low-risk disease who underwent radical prostatectomy. However, spectroscopic MRI has proven to be a superb technique for the detection

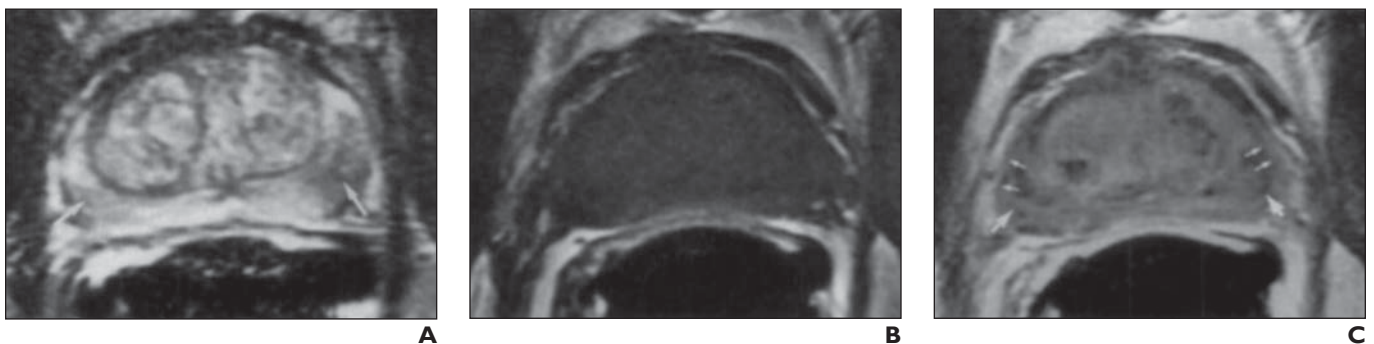


Fig. 4—63-year-old man with prostate cancer who underwent MRI for staging purposes. (Reprinted from Mirowitz SA, Brown JJ, Heiken JP. Evaluation of the prostate and prostatic carcinoma with gadolinium-enhanced endorectal coil MR imaging. *Radiology* 1993; 186:153–158, with permission from the Radiological Society of North America)

A, T2-weighted MR image (TR/TE, 2200/80) shows foci of abnormal reduced signal intensity are within peripheral zone bilaterally (arrows), corresponding to sites of cancer.

B, Unenhanced T1-weighted MR image (TR/TE, 500/25) shows prostate has uniform signal intensity.

C, Contrast-enhanced T1-weighted MR image shows inhomogeneous enhancement at sites of cancer within peripheral zone bilaterally (large arrows). Poor definition of capsular margins (small arrows) is also apparent at site with proved capsular invasion by tumor.

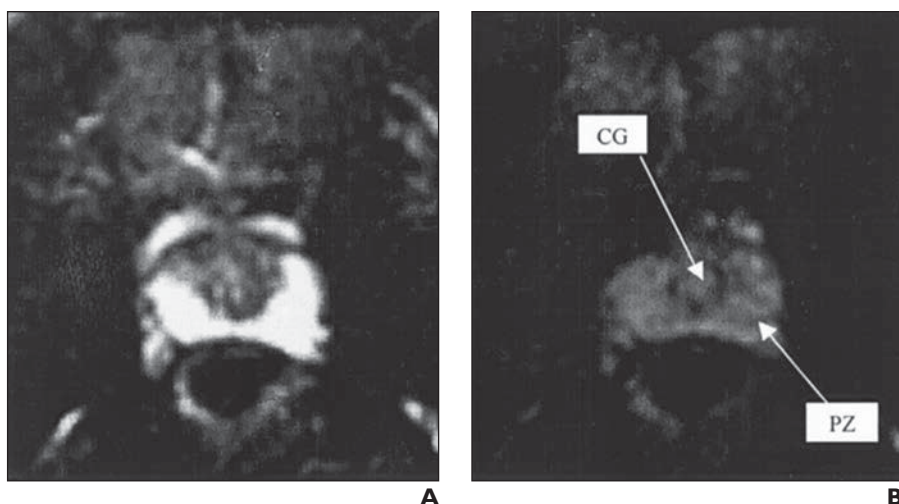


Fig. 5—Pair of diffusion-weighted echo-planar images from male volunteer. (Reprinted from Issa B. In vivo measurement of the apparent diffusion coefficient in normal and malignant prostatic tissues using echo-planar imaging. *J Magn Reson Imaging* 2002; 16:196–200. © 2002 Wiley-Liss, Inc., with permission from Wiley and Sons)

A and B, Diffusion-weighted echo-planar images obtained with b values of 0 s/mm² (**A**) and 401 s/mm² (**B**) show good contrast between different anatomic regions of gland and cover 10 × 10 cm² region because outer area was full of noise only. CG = central gland, PZ = peripheral zone.

of aggressive cancers [27–29], but DWI can now give the same information in less time and with less required expertise.

DWI—DWI shows the motion of water molecules in tissues, which is linked to tissue cellularity [30]. PCa is characterized by greater numbers of cells and destruction of water-rich glandular tissue, resulting in a lower water diffusivity (and a lower apparent diffusion coefficient [ADC]) compared with that seen in normal tissue [30]. A region of restricted diffusion (e.g., tumor) is hyperintense on high-b-value DWI and hypointense on the corresponding ADC map.

In 2002, Issa [31] was the first to report the application of DWI for PCa (Fig. 5). The ADC was measured in the transition and peripheral zones of seven healthy men and 19 men with PCa. For men with PCa, the ADCs were lower in the malignant tissue than

in noncancerous areas (1.38 vs 1.92×10^{-3} mm²/s; $p < 0.001$). Since then, many studies and reviews have investigated the usefulness of prostate DWI, supporting its inclusion in the diagnostic pathway of PCa [32–35].

Coils and Magnetic Field Strength: An Unsolved Dilemma

The first studies of prostate MRI were conducted using a conventional body coil with limited anatomic resolution [36].

In 1989, Schnall et al. [37] developed an endorectal surface coil to use when performing high-resolution prostate MRI with a 1.5-T system. Their initial experience showed that the images obtained using an endorectal coil could show prostate findings better than the images obtained using a body coil (Fig. 6).

The use of an endorectal coil was also supported in 1996 by D'Amico et al. [38],

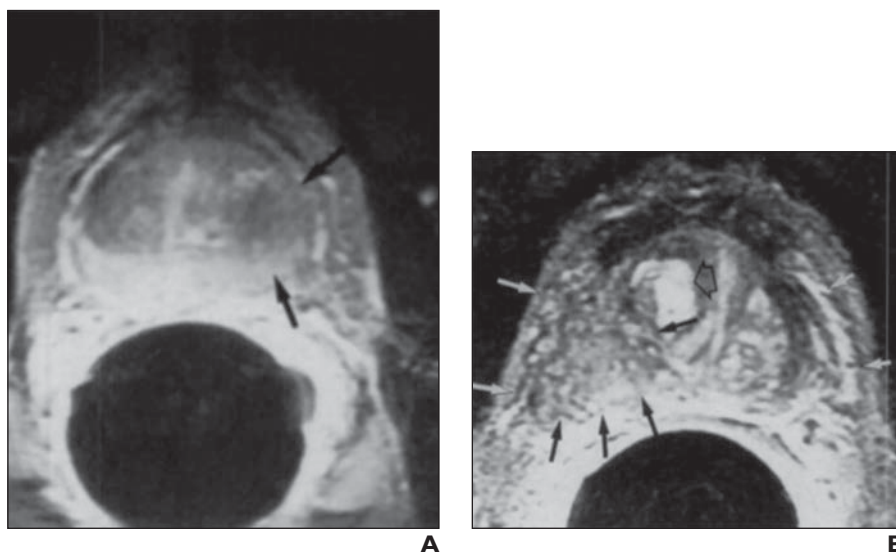
who compared the assessment of extracapsular extension and seminal vesicle invasion on MRI with the surgical specimens of 445 men. After multivariable analysis that also included clinical stage, prostate-specific antigen level, and Gleason grade, the most significant predictor of positive margins was extracapsular extension on MRI ($p = 0.001$).

From a technical point of view, the endorectal coil significantly improves the signal-to-noise ratio, resulting in higher-resolution T2-weighted imaging with an accurate delineation of the prostatic capsule, which is very important for staging. Evidence supports the use of additional endorectal coils for 1.5-T MRI, whereas the need for endorectal coils for 3-T MRI is still controversial [39–41]. Recent evidence shows that an endorectal coil at 3 T provides superior sensitivity (78%) for PCa detection, com-

Fig. 6—MR images of two patients with biopsy-proved prostate cancer. (Reprinted from Schnall MD, Lenkinski RE, Pollack HM, Imai Y, Kressel HY. Prostate: MR imaging with an endorectal surface coil. *Radiology* 1989; 172:570–574, with permission from the Radiological Society of North America)

A, Long-TR/TE (2500/80) MR image shows low-intensity lesion in left peripheral zone in region for which there were positive biopsy findings (arrows) (FOV, 16 cm²; two acquisitions).

B, Long-TR/TE (2500/80) MR image shows low-intensity lesion in right side of prostate extending into periprostatic fat (large gray arrows and large white arrows). Normal peripheral zone is not well seen on this image. Periprostatic venous plexus is obliterated by tumor on right. Normal high-signal-intensity periprostatic venous plexus is seen in left side (small gray arrows). High-signal-intensity glandular benign prostatic hyperplasia is seen in central gland (open arrow) (FOV, 12 cm²; two acquisitions).



Prostate MRI: Past, Present, and Future

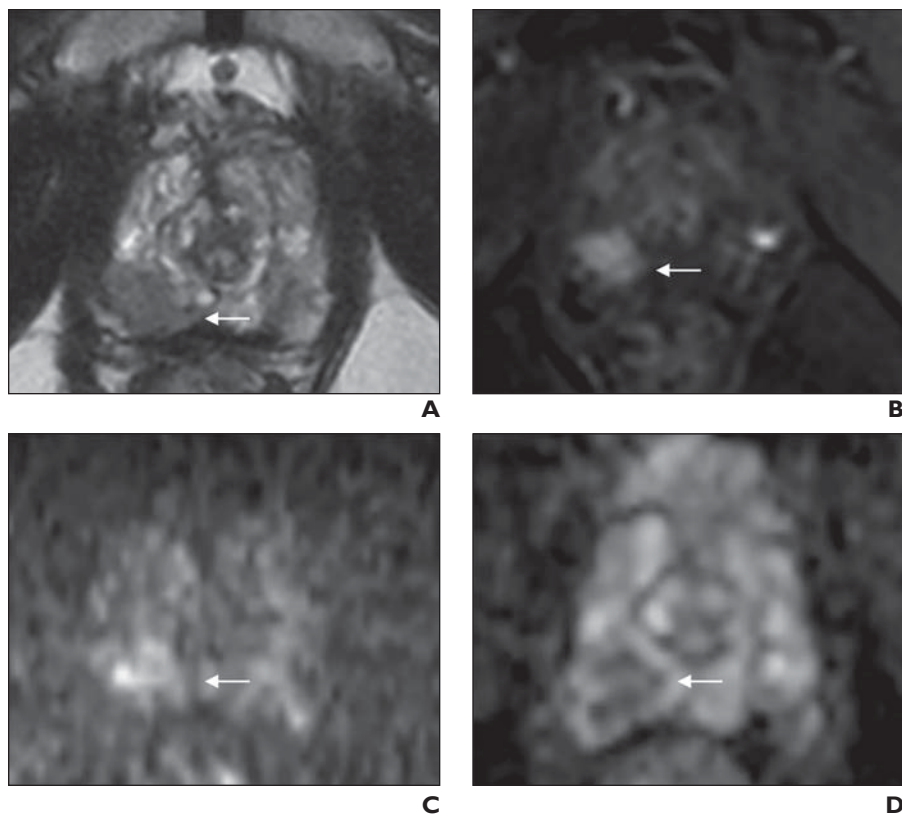


Fig. 7—71-year-old man with Gleason 3 + 4 prostate cancer who underwent multiparametric MRI of prostate performed using 3-T system without endorectal coil.

A–D, Lesion in right apex (*arrow*) is characterized by low signal intensity on T2-weighted MR image (**A**), early wash-in of contrast material on dynamic contrast-enhanced sequence (**B**), high signal intensity on DWI (b value, 2000 s/mm²) (**C**), and low signal intensity on apparent diffusion coefficient map (**D**).

pared with standard and augmented protocols (i.e., those with twice as many signal averages; 43% and 60%, respectively) with no endorectal coil ($p < 0.001$) [42]. However, the addition of an endorectal coil is associated with increases in costs, examination time, and discomfort. Moreover, each country has specific recommendations and guidelines regarding how and when to perform prostate MRI; for example, in the United Kingdom, current guidelines indicate that endorectal coils and rectal catheters for gas voiding do not need to be used routinely [43].

As far as magnet field strength is concerned, in 2004 Bloch et al. [44] reported the first comparison of 1.5- and 3-T scanners (T2-weighted imaging and DCE-MRI) with pelvic phased-array surface coils combined with an endorectal coil, confirming the higher quality and clinical utility of endorectal 3-T scanners. A 3-T MRI examination of the prostate has a higher signal-to-noise ratio and improved contrast resolution, providing more detailed images. Unfortunately, an important drawback is the high sensitivity to artifacts

(e.g., metallic artifacts from hip prostheses) that can degrade the image quality (especially that of DWI). However, in practice, these issues are generally outweighed by the benefits of using 3 T, as outlined in Prostate Imaging Reporting and Data System version 2 (PI-RADSv2) [45]. Supporting evidence indicates that 3-T MRI is able to increase the detection of smaller lesions, but the magnet strength is only one of the factors influencing acquisition of a prostate MR image of adequate image quality, as reported by Dickinson et al. [46]. The use of 1.5- or 3-T systems and endorectal coils still varies across centers, and debate is still open [47–51] (Fig. 7).

Figure 8 presents the chronologic timeline of major technical developments in MRI of the prostate.

The Present: Guidelines and Clinical Implications

Multiparametric MRI of the prostate plays an active role in assessment of the PCa clinical pathway in many countries, influencing the management of several aspects of this

disease from initial diagnosis to postrecurrence assessment. This growing interest in MRI has led to a significant heterogeneity in imaging protocols, interpretation, and implementation into clinical care [52].

Given the rapid development of the MRI technique, it is interesting to observe how and why MRI has been advocated as a valuable tool for PCa over the past decade.

First, it should be mentioned that the European Association of Urology developed a series of recommendations for PCa that were published in 2011 and were then revised [53–55]. According to these guidelines, mpMRI of the prostate should be used for local staging, specifically before repeat biopsy, when suspicion of PCa persists despite negative biopsy findings, because such a technique can change patient management and may help to trigger MRI-targeted biopsy. Whole-body DWI could be also used to assess bone metastases.

In the United Kingdom, the National Institute for Health and Care Excellence (NICE) guidelines [56] support the use of mpMRI for men with positive biopsy findings for whom radical treatment or active surveillance is being considered and for those with negative TRUS biopsy findings for whom a suspicion of PCa remains.

The American College of Radiology Appropriateness Criteria for the pretreatment detection, staging, and surveillance of PCa, released in 2013, supported the appropriateness of prostate MRI for a range of clinical scenarios [57].

Table 1 provides a more-detailed look at the key consensus studies that have involved different professional groups that are highly experienced in the field of PCa.

The first international consensus meeting on prostate MRI was published in 2011 by Dickinson et al. [46]. It was recommended that T2-weighted imaging, DWI, and DCE-MRI were the key sequences for the detection, localization, and characterization of PCa. The use of an ordinal 5-point Likert MRI-based scale to score the likelihood of malignancy (from highly unlikely to highly likely) and a pictorial report showing lesion location were recommended.

In 2012, the European Society of Urogenital Radiology (ESUR) published the first version of the Prostate Imaging Reporting and Data System (PI-RADS) [58], which included basic recommendations for MRI acquisition, interpretation, and reporting. Three different protocols (for detection, staging, and node and bone assessment) were conceived. A

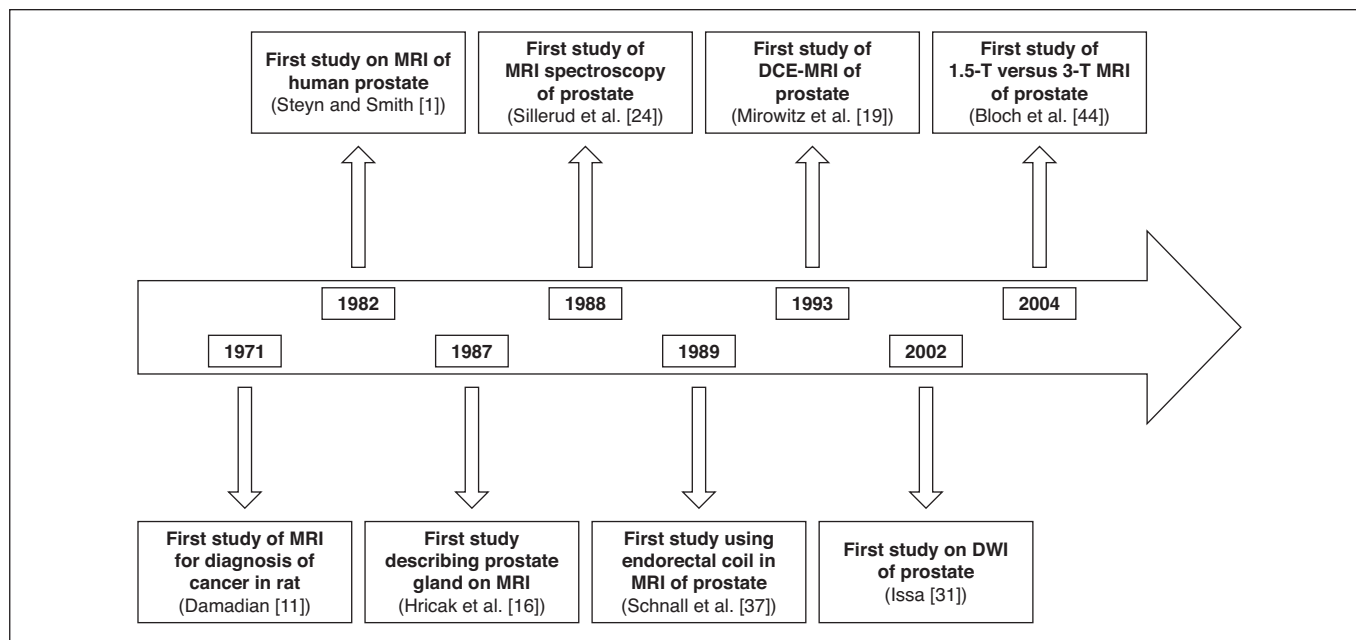


Fig. 8—Chronologic timeline of major technical developments in MRI of prostate. DCE = dynamic contrast enhanced.

score from 1 to 5 indicated the likelihood of a patient having clinically significant PCa on each MRI sequence, including spectroscopic MRI, and the overall score was then assessed. PI-RADSv2 was subsequently released in 2015 [45, 59], representing a collaborative effort of the ESUR, the American College of Radiology, and the AdMeTech Foundation. Different from PI-RADS, PI-RADSv2 simplified the interpretation of DCE-MRI and identified dominant sequences (T2-weighted sequences for the transition zone and DWI sequences for the peripheral zone) determining the overall PI-RADSv2 score. A recent meta-analysis showed a significantly higher pooled sensitivity of PI-RADSv2 compared with PI-RADS (0.95 vs 0.88, respectively; $p = 0.04$), although a similar pooled specificity was maintained (0.73 vs 0.75, respectively; $p = 0.90$) [60].

There remains a need to improve the standardization of reporting (e.g., Likert scale vs PI-RADS), but PI-RADSv2 provides a good basis from which unexperienced radiologists can interpret prostate MRI [61–63].

In 2013, another consensus meeting took place in the United Kingdom [64]. Among the recommendations from this meeting, a key message was that postbiopsy staging scans should not be acquired until at least 10 weeks after biopsy to avoid MRI artifacts. Moreover, because prostate MRI interpretation can be a challenging task for unexperienced

radiologists, and because the learning curve is steep, the authors concluded that those who report prostate MRI findings should report at least 50 scans per year and should regularly attend multidisciplinary meetings.

In 2013, Moore et al. [65] published a list of recommendations for reporting MRI-targeted biopsy studies. The panelists highlighted the importance of reporting standard and MRI-targeted biopsies separately and provided a checklist to improve the quality of reporting in MRI-targeted biopsy studies.

Growing evidence also supports the use of MRI for focal therapy [66–69]. Two important consensus meetings on this topic have stressed the importance of mpMRI and have recommended the use of MRI-targeted biopsies [70, 71].

The value of mpMRI for men with a clinical suspicion of recurrence after receiving initial treatment of PCa has been consistently shown [72]. There is robust evidence on the use of this technique for the detection and localization of recurrence after various forms of treatment, including radical prostatectomy, brachytherapy, external beam radiotherapy, focal ablation, and hormone therapy [73]. Recurrence in the prostate bed after radical prostatectomy is characterized by a soft-tissue nodule that is isointense to muscle on T1-weighted imaging, is slightly hyperintense to muscle on T2-weighted imaging, shows restricted diffusion, and, unlike post-

operative fibrosis and granulation tissue, enhances avidly after the administration of IV contrast medium [73]. Intraprostatic recurrence after radiotherapy and hormonal therapy is indicated by T2-hypointense nodular lesions with bulging of the prostatic capsule; restricted diffusion and early enhancement are also seen. When focal therapy is delivered, the use of IV contrast medium is mandatory to differentiate viable tumor from necrosis and fibrotic changes [73].

A panel of experts published the Prostate Cancer Radiologic Estimation of Change in Sequential Evaluation (PRECISE) guidelines [74] to facilitate robust data collection from serial MRI scans of men undergoing active surveillance. These recommendations were created under the assumption that a systematic approach to reporting findings from baseline and follow-up scans allows an accurate assessment of the natural history of PCa. The PRECISE recommendations include a scoring system (based on a score from 1 to 5) for identifying the likelihood of change occurring between baseline and follow-up scans; this score can facilitate the determination of thresholds for different parameters (e.g., tumor size) that identify radiologic significant disease and important radiologic changes on mpMRI. If radiologic progression is suspected, a targeted biopsy should be performed to establish that it is correlated with histologic progression [74].

Prostate MRI: Past, Present, and Future

TABLE 1: Key Consensus Studies of Prostate MRI

Study Authors [Reference]	Year of Publication	Type of Study	Location	No. of Participants	Method	Topic	Key Radiologic Message(s)
Dickinson et al. [46]	2011	Recommendations	Europe	16	Consensus meeting (RAND/UCLA appropriateness method)	Detection, localization, and characterization of prostate cancer	T2-weighted imaging, DWI, and DCE-MRI provide the key sequences 5-Point MRI-based scale for malignancy Pictorial report
Barentsz et al. [58]	2012	Guidelines (ESUR)	Europe and United States	9	Consensus meetings and e-mail discussions	PI-RADS	Guidelines to promulgate high-quality MRI scans Three protocols for detection, staging, and node and bone assessment PI-RADS classification for structured reporting
Kirkham et al. [64]	2013	Recommendations	United Kingdom	16	Consensus meeting	Detection, staging, posttreatment imaging, reporting, protocol, and training.	T2-weighted imaging, DWI, and DCE-MRI provide the key sequences High-quality 1.5-T MRI scans with pelvic phased-array coil are diagnostic MRI can be used before biopsy Staging scans performed at least 10 weeks after biopsy Standardized scoring system Pictorial report
Moore et al. [65]	2013	Recommendations	Europe, United States, and Japan	23	Consensus meeting (RAND/UCLA appropriateness method)	MRI-targeted biopsies	List of recommendations for reporting MRI-targeted biopsy studies Histologic results of standard and MRI-targeted biopsies should be reported separately using Gleason score and maximum cancer core length Checklist to improve the quality of reporting in MRI-targeted biopsy studies
van den Bos et al. [70]	2014	Recommendations	Europe and United States	13	Consensus meeting (Delphi process)	Focal therapy	In preplanning for focal therapy, T2-weighted imaging is important for assessing the anatomy, DWI for specifying lesion characteristics, and DCE-MRI for increased cancer detection MRI should be performed before biopsies (or at least 6–8 weeks afterward) and should be assessed by trained urologists

(Table 1 continues on next page)

TABLE 1: Key Consensus Studies of Prostate MRI (continued)

Study Authors [Reference]	Year of Publication	Type of Study	Location	No. of Participants	Method	Topic	Key Radiologic Message(s)
Donaldson et al. [71]	2015	Recommendations	Europe and United States	15	Consensus meeting (RAND/UCLA appropriateness method)	Focal therapy	Focal therapy can be performed for men who have undergone an MRI-targeted prostate biopsy and for men who have undergone standard TRUS-guided biopsy with findings concordant with those of high-quality MR image reported by an expert radiologist When MRI-targeted strategy is used, the START guidelines should be followed DWI is the dominant sequence for peripheral zone lesions
Weinreb et al. [45]	2016	Guidelines	Europe, United States, and Canada	Steering Committee (ACR, ESUR, and AdMeTech Foundation)	Expert consensus opinion	PI-RADSv2	T2-weighted imaging is the dominant sequence for transition zone lesions DCE-MRI scoring is simplified to negative or positive findings Thirty-nine-sector map for lesion localization
Moore et al. [74]	2017	Recommendations	Europe, United States, and Canada	19	Consensus meeting (RAND/UCLA appropriateness method)	Active surveillance	Development of a PRECISE scoring system (scale, 1–5) for serial MR images Reporting the index lesion size using absolute values at baseline and follow-up
Padhani et al. [75]	2017	Recommendations	Europe and United States	13	Review by experts	Metastatic disease	Checklist of items for reporting a cohort of men on active surveillance METastasis Reporting and Data System for Prostate Cancer represents the consensus recommendations on the performance, quality standards, and reporting of whole-body MRI, for use in advanced prostate cancer These new criteria require validation in clinical trials

(Table 1 continues on next page)

Prostate MRI: Past, Present, and Future

TABLE 1: Key Consensus Studies of Prostate MRI (continued)

Study Authors [Reference]	Year of Publication	Type of Study	Location	No. of Participants	Method	Topic	Key Radiologic Message(s)
Fulgham et al. [76]	2017	Recommendations	United States	9	Critical review and collective expert opinion	Diagnosis, staging, and management of prostate cancer	MRI can be used for men with abnormal findings on digital rectal examination or an elevated PSA level and a previous negative biopsy result Insufficient evidence to recommend MRI for screening or surveillance of prostate cancer
Brizhohun Appayya et al. [43]	2018	Recommendations	United Kingdom	15	Consensus meeting (RAND/UCLA appropriateness method)	Diagnosis, staging, and management of prostate cancer	Prostate MRI requests should be made in consultation with the urologic team
Padhani et al. [59]	2019	Guidelines (update)	Europe and United States	6	International experts	This study was intended to discuss the current status and future directions of PI-RADSv2.	Quality assessment checks of MRI scanners to guarantee scans of consistently high diagnostic quality Scans should be reported by trained and experienced radiologists only Robust evidence that mpMRI can detect and localize clinically significant prostate cancer Recognition of widespread implementation of PI-RADSv2 Need for more robust data supporting the use of MRI for biopsy-naïve men

Note — RAND = RAND Corporation, UCLA = University of California, Los Angeles, DCE = dynamic contrast-enhanced, ESUR = European Society of Urogenital Radiology, PI-RADS = Prostate Imaging Reporting and Data System, TRUS = transrectal ultrasound, START = standards of reporting for MRI-targeted biopsy studies, ACR = American College of Radiology, PRECISE = Prostate Cancer Radiologic Estimation of Change in Sequential Evaluation, PSA = prostate-specific antigen, mpMRI = multiparametric MRI, PI-RADSv2 = Prostate Imaging Reporting and Data System version 2.

Once PCa is diagnosed, it is also crucial to determine whether the cancer has spread beyond the prostate capsule, because prognosis and treatment options differ between organ-confined and locally advanced or metastatic disease. In 2016, an international expert panel of oncologic imagers and oncologists [75] drafted the METastasis Reporting and Data System for Prostate Cancer guidelines. Such recommendations were built to promote standardization and diminish variation in the acquisition, interpretation, and reporting of whole-body MRI scans in advanced PCa and to provide comprehensive tumor characterization both before treatment and over time [75].

In 2017, the American Urologic Association statement on the use of mpMRI for PCa [76] endorsed the use of mpMRI for men with abnormal digital rectal examination findings or an elevated prostate-specific antigen level and a previous negative biopsy finding, but it also highlighted that mpMRI cannot yet be recommended for screening or surveillance. The results from a recent consensus meeting to implement mpMRI in the diagnostic pathway of PCa in the United Kingdom has been published, with a set of criteria required for the practical dissemination of high-quality mpMRI as a diagnostic test before biopsy in men at risk for PCa [43]. In this regard, the National Health Service (NHS) of England recommends that all men with suspected PCa should have PCa diagnosed within 28 days at most, with mpMRI performed before biopsy [77].

Future Directions

Currently, prostate mpMRI is in a very interesting phase. As shown in the previous sections of this article, remarkable advances have been made over the past decades. The primary goal remains the correct identification of clinically significant PCa, ensuring the most accurate histologic diagnosis by targeted biopsy [4].

In countries like the United Kingdom, widespread use of mpMRI before biopsy already exists across different settings [77, 78]. However, many challenges still have to be addressed, and these challenges have been recently outlined in a consensus meeting [43]. In other countries, such as the United States, debate on the usefulness and cost-effectiveness of prostate mpMRI continues [76]. The American Urologic Association guidelines recommend that scans be obtained at dedicated high-quality centers, which quite often are academic centers [76]. Therefore, the reproducibility of high-quality prostate MRI outside such institutions remains a big challenge, and results are often difficult to generalize. To address this issue, the PROMIS and PRECISION trials deliberately involved aca-

demic and nonacademic centers using different MRI systems [3, 4].

The PROMIS trial [3] compared the performance of mpMRI with that of TRUS-guided biopsy in 576 biopsy-naïve men, with use of a 5-mm-template transperineal biopsy as reference standard and with a negative predictive value of 89% for a Gleason score of 4 + 3 or higher or a cancer core length of 6 mm or higher. An MRI examination with negative findings did not miss any primary Gleason pattern 4 disease, but the negative predictive value was 76% when a Gleason score of 3 + 4 or higher was considered (compared with a negative predictive value of 63% when TRUS-guided biopsy was performed).

The PRECISION trial [4] has shown the superior accuracy of MRI-targeted biopsy alone compared with TRUS-guided biopsy, with targeted biopsies alone detecting more clinically significant cancer than TRUS-guided biopsies (38% vs 26%) and fewer insignificant cancers (9% vs 22%). The negative predictive value of MRI was recently shown by Panebianco et al. [79], who assessed the value of an MRI scan with negative findings in 1545 patients after 48 months of follow-up. For patients with clinically significant cancer, the probability of diagnosis-free survival at 48 months was 95% for biopsy-naïve men and 96% for men with previous negative biopsy findings. Similar findings apply to men undergoing active surveillance [80]. Further studies defining radiologic progression according to the PRECISE guidelines are needed [74].

In recent years, there has been also considerable interest in the debate concerning biparametric MRI (i.e., without DCE imaging) vs mpMRI [81], with initial evidence supporting the use of biparametric MRI in given settings [82–84]. However, large, multicenter and prospective trials will need to be undertaken to confirm these initial results. It has also been shown that an MRI-based pathway can be cost-effective in different settings, both when MRI is the triage test before performing any type of biopsy or when the goal is to avoid such an invasive procedure [85–88].

In addition to the differences in referring patients or associated costs (for public vs private health care systems), a plethora of different vendors, MRI scanners, and platforms is currently available on the market, and this should be always borne in mind. Radiologic training in prostate mpMRI reporting should also be considered because evidence sup-

ports the presence of a steep learning curve for beginners, especially when imaging tumors in the transition zone [89–93].

Different scanners with different magnet strengths have generated a large variability in the selection of MRI acquisition parameters, especially in terms of the b values used for DWI. There is evidence supporting the use of high b values at 3 T to increase the accuracy of PCa detection, but future studies should aim at standardizing data acquisition protocols [94, 95].

There is interest in applying artificial intelligence to save time and improve diagnosis of PCa by using mpMRI. However, actual clinical benefits are not yet definitively established. In particular, computer-aided diagnosis systems and quantitative imaging are two promising fields in prostate mpMRI, with growing evidence supporting the use of computer-aided diagnosis systems and imaging biomarkers (e.g., the ADC) in the management of PCa [96–102].

Greer et al. [96] showed that computer-aided diagnosis improves sensitivity for index lesions (from 78% to 86%; $p = 0.013$), compared with mpMRI alone, and it also improves the agreement between different radiologists in detecting a lesion (57% vs 72%; $p < 0.001$).

Bonekamp et al. [97] compared biparametric (i.e., unenhanced) radiomic machine learning, the mean ADC, and the radiologic clinical assessment for the characterization of clinically significant PCa (denoted by a Gleason grade group ≥ 2) on mpMRI. The radiologist had a per-lesion sensitivity of 88% and specificity of 50%, whereas quantitative measurement of the mean ADC (cutoff, 732 mm^2/s) significantly reduced false-positive and false-negative findings for lesions, with a sensitivity of 90% and specificity of 62% ($p = 0.048$). In per-patient analysis, the radiologist had a sensitivity and specificity of 89% and 43%, respectively, whereas the mean ADC had a sensitivity and specificity of 93% and 51%, respectively ($p = 0.496$). No added benefit of radiomic machine learning was present when mean ADC values were used alone.

Although these early results are encouraging, continued research is required.

Conclusion

Over the past decades, remarkable advances in MRI for PCa have been made, and several data support the role of this technique for PCa. Because the number of institutions

adopting prostate mpMRI as a diagnostic tool is growing, it is vital to minimize the variability of scan quality across different centers and scanners and reduce interobserver variability between reporting radiologists.

References

1. Steyn JH, Smith FW. Nuclear magnetic resonance imaging of the prostate. *Br J Urol* 1982; 54:726–728
2. Edelman RR. The history of MR imaging as seen through the pages of *Radiology*. *Radiology* 2014; 273(2S):S181–S200
3. Ahmed HU, El-Shater Bosaily A, Brown LC, et al.; PROMIS study group. Diagnostic accuracy of multi-parametric MRI and TRUS biopsy in prostate cancer (PROMIS): a paired validating confirmatory study. *Lancet* 2017; 389:815–822
4. Kasivisvanathan V, Rannikko AS, Borghi M, et al.; PRECISION Study Group Collaborators. MRI-targeted or standard biopsy for prostate-cancer diagnosis. *N Engl J Med* 2018; 378:1767–1777
5. Loeb S, Bjurlin MA, Nicholson J, et al. Overdiagnosis and overtreatment of prostate cancer. *Eur Urol* 2014; 65:1046–1055
6. Schröder FH, Hugosson J, Roobol MJ, et al.; ERSPC Investigators. Screening and prostate cancer mortality: results of the European Randomised Study of Screening for Prostate Cancer (ERSPC) at 13 years of follow-up. *Lancet* 2014; 384:2027–2035
7. Costa DN, Pedrosa I, Donato F Jr, Roehrborn CG, Rofsky NM. MR imaging–transrectal US fusion for targeted prostate biopsies: implications for diagnosis and clinical management. *RadioGraphics* 2015; 35:696–708
8. Takahashi H, Ouchi T. The ultrasonic diagnosis in the field of urology. *Proc Jpn Soc Ultrason Med* 1963; 3:7
9. Watanabe H, Kaiho H, Tanaka M, Terasawa Y. Diagnostic application of ultrasonotomography to the prostate. *Invest Urol* 1971; 8:548–559
10. Price JM, Davidson AJ. Computed tomography in the evaluation of the suspected carcinomatous prostate. *Urol Radiol* 1979; 1:39–42
11. Damadian R. Tumor detection by nuclear magnetic resonance. *Science* 1971; 171:1151–1153
12. Hricak H, Williams RD, Spring DB, et al. Anatomy and pathology of the male pelvis by magnetic resonance imaging. *AJR* 1983; 141:1101–1110
13. Bryan PJ, Butler HE, LiPuma JP, et al. NMR scanning of the pelvis: initial experience with a 0.3 T system. *AJR* 1983; 141:1111–1118
14. Buonocore E, Hesemann C, Pavlicek W, Montie JE. Clinical and in vitro magnetic resonance imaging of prostatic carcinoma. *AJR* 1984; 143:1267–1272
15. Poon PY, McCallum RW, Henkelman MM, et al. Magnetic resonance imaging of the prostate.

Prostate MRI: Past, Present, and Future

- Radiology* 1985; 154:143–149
16. Hricak H, Dooms GC, McNeal JE, et al. MR imaging of the prostate gland: normal anatomy. *AJR* 1987; 148:51–58
 17. Dickinson L, Ahmed HU, Allen C, et al.; PREDICT Consensus Panel. Clinical applications of multiparametric MRI within the prostate cancer diagnostic pathway. *Urol Oncol* 2013; 31:281–284
 18. Cornud F, Delongchamps NB, Mozer P, et al. Value of multiparametric MRI in the work-up of prostate cancer. *Curr Urol Rep* 2012; 13:82–92
 19. Mirowitz SA, Brown JJ, Heiken JP. Evaluation of the prostate and prostatic carcinoma with gadolinium-enhanced endorectal coil MR imaging. *Radiology* 1993; 186:153–157
 20. Brown G, Macvicar DA, Ayton V, Husband JE. The role of intravenous contrast enhancement in magnetic resonance imaging of prostatic carcinoma. *Clin Radiol* 1995; 50:601–606
 21. Franiel T, Hamm B, Hricak H. Dynamic contrast-enhanced magnetic resonance imaging and pharmacokinetic models in prostate cancer. *Eur Radiol* 2011; 21:616–626
 22. Bonekamp D, Macura KJ. Dynamic contrast-enhanced magnetic resonance imaging in the evaluation of the prostate. *Top Magn Reson Imaging* 2008; 19:273–284
 23. Kayhan A, Fan X, Oto A. Dynamic contrast-enhanced magnetic resonance imaging in prostate cancer. *Top Magn Reson Imaging* 2009; 20:105–112
 24. Sillerud LO, Halliday KR, Griffey RH, Fenoglio-Preiser C, Sheppard S. In vivo ¹³C NMR spectroscopy of the human prostate. *Magn Reson Med* 1988; 8:224–230
 25. Kurhanewicz J, Vigneron DB, Nelson SJ, et al. Citrate as an in vivo marker to discriminate prostate cancer from benign prostatic hyperplasia and normal prostate peripheral zone: detection via localized proton spectroscopy. *Urology* 1995; 45:459–466
 26. Weinreb JC, Blume JD, Coakley FV, et al. Prostate cancer: sextant localization at MR imaging and MR spectroscopic imaging before prostatectomy: results of ACRIN prospective multi-institutional clinicopathologic study. *Radiology* 2009; 251:122–133
 27. Mowatt G, Scotland G, Boachie C, et al. The diagnostic accuracy and cost-effectiveness of magnetic resonance spectroscopy and enhanced magnetic resonance imaging techniques in aiding the localisation of prostate abnormalities for biopsy: a systematic review and economic evaluation. *Health Technol Assess* 2013; 17:vii–xix, 1–281
 28. Villeirs GM, De Meerleer GO, De Visschere PJ, Fonteyne VH, Verbaeys AC, Oosterlinck W. Combined magnetic resonance imaging and spectroscopy in the assessment of high grade prostate carcinoma in patients with elevated PSA: a single-institution experience of 356 patients. *Eur J Radiol* 2011; 77:340–345
 29. Umbehr M, Bachmann LM, Held U, et al. Combined magnetic resonance imaging and magnetic resonance spectroscopy imaging in the diagnosis of prostate cancer: a systematic review and meta-analysis. *Eur Urol* 2009; 55:575–590
 30. Chatterjee A, Watson G, Myint E, Sved P, McEntee M, Bourne R. Changes in epithelium, stroma, and lumen space correlate more strongly with Gleason pattern and are stronger predictors of prostate ADC changes than cellularity metrics. *Radiology* 2015; 277:751–762
 31. Issa B. In vivo measurement of the apparent diffusion coefficient in normal and malignant prostatic tissues using echo-planar imaging. *J Magn Reson Imaging* 2002; 16:196–200
 32. Tan CH, Wang J, Kundra V. Diffusion weighted imaging in prostate cancer. *Eur Radiol* 2011; 21:593–603
 33. Jie C, Rongbo L, Ping T. The value of diffusion-weighted imaging in the detection of prostate cancer: a meta-analysis. *Eur Radiol* 2014; 24:1929–1941
 34. Jacobs MA, Ouwerkerk R, Petrowski K, Macura KJ. Diffusion-weighted imaging with apparent diffusion coefficient mapping and spectroscopy in prostate cancer. *Top Magn Reson Imaging* 2008; 19:261–272
 35. Gibbs P, Pickles MD, Turnbull LW. Diffusion imaging of the prostate at 3.0 Tesla. *Invest Radiol* 2006; 41:185–188
 36. Bezzi M, Kressel HY, Allen KS, et al. Prostatic carcinoma: staging with MR imaging at 1.5 T. *Radiology* 1988; 169:339–346
 37. Schnall MD, Lenkinski RE, Pollack HM, Imai Y, Kressel HY. Prostate: MR imaging with an endorectal surface coil. *Radiology* 1989; 172:570–574
 38. D'Amico AV, Whittington R, Malkowicz SB, et al. Critical analysis of the ability of the endorectal coil magnetic resonance imaging scan to predict pathologic stage, margin status, and postoperative prostate-specific antigen failure in patients with clinically organ-confined prostate cancer. *J Clin Oncol* 1996; 14:1770–1777
 39. Heijmink SWTPJ, Fütterer JJ, Hambrock T, et al. Prostate cancer: body-array versus endorectal coil MR imaging at 3 T: comparison of image quality, localization, and staging performance. *Radiology* 2007; 244:184–195
 40. Engelbrecht MR, Jager GJ, Laheij RJ, Verbeek AL, van Lier HJ, Barentsz JO. Local staging of prostate cancer using magnetic resonance imaging: a meta-analysis. *Eur Radiol* 2002; 12:2294–2302
 41. Gawlitza J, Reiss-Zimmermann M, Thörmer G, et al. Impact of the use of an endorectal coil for 3 T prostate MRI on image quality and cancer detection rate. *Sci Rep* 2017; 7:40640
 42. Costa DN, Yuan Q, Xi Y, et al. Comparison of prostate cancer detection at 3-T MRI with and without an endorectal coil: a prospective, paired-patient study. *Urol Oncol* 2016; 34:255.e7–255.e13
 43. Brizmohun Appayya M, Adsheed J, Ahmed HU, et al. National implementation of multi-parametric magnetic resonance imaging for prostate cancer detection: recommendations from a UK consensus meeting. *BJU Int* 2018; 122:13–25
 44. Bloch BN, Rofsky NM, Baroni RH, Marquis RP, Pedrosa I, Lenkinski RE. 3 Tesla magnetic resonance imaging of the prostate with combined pelvic phased-array and endorectal coils: initial experience(1). *Acad Radiol* 2004; 11:863–867
 45. Weinreb JC, Barentsz JO, Choyke PL, et al. PI-RADS Prostate Imaging - Reporting and Data System: 2015, version 2. *Eur Urol* 2016; 69:16–40
 46. Dickinson L, Ahmed HU, Allen C, et al. Magnetic resonance imaging for the detection, localisation, and characterisation of prostate cancer: recommendations from a European consensus meeting. *Eur Urol* 2011; 59:477–494
 47. Kim CK, Park BK. Update of prostate magnetic resonance imaging at 3 T. *J Comput Assist Tomogr* 2008; 32:163–172
 48. Kim CK, Park BK, Kim B. Diffusion-weighted MRI at 3 T for the evaluation of prostate cancer. *AJR* 2010; 194:1461–1469
 49. Beyersdorff D, Taymoorian K, Knösel T, et al. MRI of prostate cancer at 1.5 and 3.0 T: comparison of image quality in tumor detection and staging. *AJR* 2005; 185:1214–1220
 50. Cornfeld DM, Weinreb JC. MR imaging of the prostate: 1.5T versus 3T. *Magn Reson Imaging Clin N Am* 2007; 15:433–448, viii
 51. Fütterer JJ, Barentsz JO, Heijmink SW. Value of 3-T magnetic resonance imaging in local staging of prostate cancer. *Top Magn Reson Imaging* 2008; 19:285–289
 52. Wollin DA, Makarov DV. Guideline of guidelines: imaging of localized prostate cancer. *BJU Int* 2015; 116:526–530
 53. Heidenreich A, Bellmunt J, Bolla M, et al.; European Association of Urology. EAU guidelines on prostate cancer. Part 1. Screening, diagnosis, and treatment of clinically localised disease. *Eur Urol* 2011; 59:61–71
 54. Heidenreich A, Bastian PJ, Bellmunt J, et al.; European Association of Urology. EAU guidelines on prostate cancer. part 1: screening, diagnosis, and local treatment with curative intent-update 2013. *Eur Urol* 2014; 65:124–137
 55. Mottet N, Van den Bergh RCN, Briers E, et al. EAU-ESTRO-ESUR-SIOG Guidelines on Prostate Cancer. European Association of Urology website. uroweb.org/wp-content/uploads/EAU-ESTRO-ESUR-SIOG-Guidelines-on-Prostate-Cancer-large-text-V2.pdf. Published 2018. Ac-

- cessed March 8, 2019
56. National Institute for Health and Care Excellence (NICE). Prostate cancer: diagnosis and management. Clinical guideline [CG175]. NICE website. www.nice.org.uk/guidance/CG175. Published January 2014. Accessed March 8 2019
 57. Eberhardt SC, Carter S, Casalino DD, et al. ACR Appropriateness Criteria prostate cancer: pretreatment detection, staging, and surveillance. *J Am Coll Radiol* 2013; 10:83–92
 58. Barentsz JO, Richenberg J, Clements R, et al.; European Society of Urogenital Radiology. ESUR prostate MR guidelines 2012. *Eur Radiol* 2012; 22:746–757
 59. Padhani AR, Weinreb J, Rosenkrantz AB, Villeirs G, Turkbey B, Barentsz J. Prostate Imaging-Reporting and Data System Steering Committee: PI-RADS v2 status update and future directions. *Eur Urol* 2019; 75:385–396
 60. Woo S, Suh CH, Kim SY, Cho JY, Kim SH. Diagnostic performance of prostate imaging reporting and data system version 2 for detection of prostate cancer: a systematic review and diagnostic meta-analysis. *Eur Urol* 2017; 72:177–188
 61. Renard-Penna R, Mozer P, Cornud F, et al. Prostate Imaging Reporting and Data System and Likert scoring system: multiparametric MR imaging validation study to screen patients for initial biopsy. *Radiology* 2015; 275:458–468
 62. Brizmohun Appayya M, Sidhu HS, Dikaios N, et al. Characterizing indeterminate (Likert-score 3/5) peripheral zone prostate lesions with PSA density, PI-RADS scoring and qualitative descriptors on multiparametric MRI. *Br J Radiol* 2018; 91:20170645
 63. Rosenkrantz AB, Kim S, Lim RP, et al. Prostate cancer localization using multiparametric MR imaging: comparison of Prostate Imaging Reporting and Data System (PI-RADS) and Likert scales. *Radiology* 2013; 269:482–492
 64. Kirkham APS, Haslam P, Keanie JY, et al. Prostate MRI: who, when, and how? Report from a UK consensus meeting. *Clin Radiol* 2013; 68:1016–1023
 65. Moore CM, Kasivisvanathan V, Eggen S, et al.; START Consortium. Standards of reporting for MRI-targeted biopsy studies (START) of the prostate: recommendations from an International Working Group. *Eur Urol* 2013; 64:544–552
 66. Nour SGMR. MR imaging-guided focal treatment of prostate cancer: an update. *Radiol Clin North Am* 2018; 56:301–318
 67. Lindner U, Lawrentschuk N, Trachtenberg J. Image guidance for focal therapy of prostate cancer. *World J Urol* 2010; 28:727–734
 68. Wysock JS, Lepor H. Multi-parametric MRI imaging of the prostate-implications for focal therapy. *Transl Androl Urol* 2017; 6:453–463
 69. Oto A, Sethi I, Karczmar G, et al. MR imaging-guided focal laser ablation for prostate cancer: phase I trial. *Radiology* 2013; 267:932–940
 70. van den Bos W, Muller BG, Ahmed H, et al. Focal therapy in prostate cancer: international multidisciplinary consensus on trial design. *Eur Urol* 2014; 65:1078–1083
 71. Donaldson IA, Alonzi R, Barratt D, et al. Focal therapy: patients, interventions, and outcomes—a report from a consensus meeting. *Eur Urol* 2015; 67:771–777
 72. De Visschere P, Vargas HA, Ost P, De Meerleer GO, Villeirs GM. Imaging treated prostate cancer. *Abdom Imaging* 2013; 38:1431–1446
 73. Vargas HA, Wassberg C, Akin O, Hricak H. MR imaging of treated prostate cancer. *Radiology* 2012; 262:26–42
 74. Moore CM, Giganti F, Albertsen P, et al. Reporting magnetic resonance imaging in men on active surveillance for prostate cancer: the PRECISE recommendations—a report of a European school of oncology task force. *Eur Urol* 2017; 71:648–655
 75. Padhani AR, Lecouvet FE, Tunariu N, et al. METastasis Reporting and Data System for Prostate Cancer: practical guidelines for acquisition, interpretation, and reporting of whole-body magnetic resonance imaging-based evaluations of multiorgan involvement in advanced prostate cancer. *Eur Urol* 2017; 71:81–92
 76. Fulgham PF, Rukstalis DB, Turkbey IB, et al. AUA policy statement on the use of multiparametric magnetic resonance imaging in the diagnosis, staging and management of prostate cancer. *J Urol* 2017; 198:832–838
 77. National Health Service England. National Institute for Health and Care Excellence (NICE) guidelines. www.england.nhs.uk/wp-content/uploads/2018/04/implementing-timed-prostate-cancer-diagnostic-pathway.pdf. Published April 18, 2018. Accessed October 4, 2018
 78. Moore C. Can negative prostate magnetic resonance imaging give us the reassurance we need to avoid standard biopsy? An evidence-based practical approach. *Eur Urol* 2018; 74:55–56
 79. Panebianco V, Barchetti G, Simone G, et al. Negative multiparametric magnetic resonance imaging for prostate cancer: what's next? *Eur Urol* 2018; 74:48–54
 80. Moore CM, Petrides N, Emberton M. Can MRI replace serial biopsies in men on active surveillance for prostate cancer? *Curr Opin Urol* 2014; 24:280–287
 81. Puech P, Sufana-Iancu A, Renard B, Lemaitre L. Prostate MRI: can we do without DCE sequences in 2013? *Diagn Interv Imaging* 2013; 94:1299–1311
 82. Woo S, Suh CH, Kim SY, Cho JY, Kim SH, Moon MH. Head-to-head comparison between biparametric and multiparametric MRI for the diagnosis of prostate cancer: a systematic review and meta-analysis. *AJR* 2018; 211:[web]W226–W241
 83. Niu XK, Chen ZF, Chen L, Li J, Peng T, Li X. Clinical application of biparametric MRI texture analysis for detection and evaluation of high-grade prostate cancer in zone-specific regions. *AJR* 2018; 210:549–556
 84. Boesen L, Nørgaard N, Løgager V, et al. Assessment of the diagnostic accuracy of biparametric magnetic resonance imaging for prostate cancer in biopsy-naive men: the Biparametric MRI for Detection of Prostate Cancer (BIDOC) study. *JAMA Netw Open* 2018; 1:e180219
 85. Pepe P, Pepe G, Pepe L, Garufi A, Priolo GD, Pennisi M. Cost-effectiveness of multiparametric MRI in 800 men submitted to repeat prostate biopsy: results of a public health model. *Anticancer Res* 2018; 38:2395–2398
 86. Barnett CL, Davenport MS, Montgomery JS, Wei JT, Montie JE, Denton BT. Cost-effectiveness of magnetic resonance imaging and targeted fusion biopsy for early detection of prostate cancer. *BJU Int* 2018; 122:50–58
 87. Cerantola Y, Dragomir A, Tanguay S, Bladou F, Aprikian A, Kassouf W. Cost-effectiveness of multiparametric magnetic resonance imaging and targeted biopsy in diagnosing prostate cancer. *Urol Oncol* 2016; 34:119.e1–119.e9
 88. Panebianco V, Valerio MC, Giuliani A, et al. Clinical utility of multiparametric magnetic resonance imaging as the first-line tool for men with high clinical suspicion of prostate cancer. *Eur Urol Oncol* 2018; 1:208–214
 89. Rosenkrantz AB, Begovic J, Pires A, Won E, Taneja SS, Babb JS. Online interactive case-based instruction in prostate magnetic resonance imaging interpretation using Prostate Imaging and Reporting Data System version 2: effect for novice readers. *Curr Probl Diagn Radiol* 2018; 48:132–141
 90. Akin O, Riedl CC, Ishill NM, Moskowitz CS, Zhang J, Hricak H. Interactive dedicated training curriculum improves accuracy in the interpretation of MR imaging of prostate cancer. *Eur Radiol* 2010; 20:995–1002
 91. Rosenkrantz AB, Ginocchio LA, Cornfeld D, et al. Interobserver reproducibility of the PI-RADS version 2 lexicon: a multicenter study of six experienced prostate radiologists. *Radiology* 2016; 280:793–804
 92. Rosenkrantz AB, Ayoola A, Hoffman D, et al. The learning curve in prostate MRI interpretation: self-directed learning versus continual reader feedback. *AJR* 2017; 208:[web]W92–W100
 93. Garcia-Reyes K, Passoni NM, Palmeri ML, et al. Detection of prostate cancer with multiparametric MRI (mpMRI): effect of dedicated reader

Prostate MRI: Past, Present, and Future

- education on accuracy and confidence of index and anterior cancer diagnosis. *Abdom Imaging* 2015; 40:134–142
94. Manenti G, Nezzo M, Chegai F, Vasili E, Bonanno E, Simonetti G. DWI of prostate cancer: optimal b-value in clinical practice. *Prostate Cancer* 2014; 2014:868269
95. Tamada T, Kanomata N, Sone T, et al. High b value (2,000 s/mm²) diffusion-weighted magnetic resonance imaging in prostate cancer at 3 Tesla: comparison with 1,000 s/mm² for tumor conspicuity and discrimination of aggressiveness. *PLoS One* 2014; 9:e96619
96. Greer MD, Lay N, Shih JH, et al. Computer-aided diagnosis prior to conventional interpretation of prostate mpMRI: an international multi-reader study. *Eur Radiol* 2018; 28:4407–4417
97. Bonekamp D, Kohl S, Wiesenfarth M, et al. Radiomic machine learning for characterization of prostate lesions with MRI: comparison to ADC values. *Radiology* 2018; 289:128–137
98. Choyke PL. Quantitative MRI or machine learning for prostate MRI: which should you use? *Radiology* 2018; 289:138–139
99. Valerio M, Zini C, Fierro D, et al. 3T multiparametric MRI of the prostate: does intravoxel incoherent motion diffusion imaging have a role in the detection and stratification of prostate cancer in the peripheral zone? *Eur J Radiol* 2016; 85:790–794
100. Nguyen TB, Ushinsky A, Yang A, et al. Utility of quantitative apparent diffusion coefficient measurements and normalized apparent diffusion coefficient ratios in the diagnosis of clinically significant peripheral zone prostate cancer. *Br J Radiol* 2018; 91:20180091
101. Hoang Dinh A, Melodelima C, Souchon R, et al. Quantitative analysis of prostate multiparametric MR images for detection of aggressive prostate cancer in the peripheral zone: a multiple imager study. *Radiology* 2016; 280:117–127
102. Metzger GJ, Kalavagunta C, Spilseth B, et al. Detection of prostate cancer: quantitative multiparametric MR imaging models developed using registered correlative histopathology. *Radiology* 2016; 279:805–816